Original Article

Regulatory mechanisms of haptoglobin on particulate matter-induced epithelial-to-mesenchymal transition in bronchial epithelial cells

Yao Qian[1,2#], Chenchen Fang[3#], Beibei Wang[1], Zhixiao Xu[1], Wenkai Yu[4], Andrei I. Gritsiuta[5], Chengshui Chen[1,6], Nian Dong[1], Junjie Chen[1]

[1]Key Laboratory of Interventional Pulmonology of Zhejiang Province, Department of Pulmonary and Critical Care Medicine, The First Affiliated Hospital of Wenzhou Medical University, Wenzhou, China; [2]Department of Pathology, Taizhou Central Hospital (Taizhou University Hospital), Taizhou, China; [3]Emergency Department, The First Affiliated Hospital of Wenzhou Medical University, Wenzhou, China; [4]Wenzhou Medical University, Wenzhou, China; [5]Department of Surgery, University of Pittsburgh Medical Center, Pittsburgh, PA, USA; [6]Zhejiang Province Engineering Research Center for Endoscope Instruments and Technology Development, Department of Pulmonary and Critical Care Medicine, Quzhou People's Hospital, The Quzhou Affiliated Hospital of Wenzhou Medical University, Quzhou, China

Contributions: (I) Conception and design: C Chen, N Dong, J Chen; (II) Administrative support: N Dong, J Chen; (III) Provision of study materials or patients: B Wang, Z Xu; (IV) Collection and assembly of data: N Dong, J Chen; (V) Data analysis and interpretation: Y Qian, C Fang, B Wang, W Yu, Z Xu, AI Gritsiuta; (VI) Manuscript writing: All authors; (VII) Final approval of manuscript: All authors.

[#]These authors contributed equally to this work.

Correspondence to: Chengshui Chen, PhD. Key Laboratory of Interventional Pulmonology of Zhejiang Province, Department of Pulmonary and Critical Care Medicine, The First Affiliated Hospital of Wenzhou Medical University, Shangcai Village, Ouhai District, Wenzhou 325000, China; Zhejiang Province Engineering Research Center for Endoscope Instruments and Technology Development, Department of Pulmonary and Critical Care Medicine, Quzhou People's Hospital, The Quzhou Affiliated Hospital of Wenzhou Medical University, Kecheng District, Quzhou 324000, China. Email: chenchengshui@wmu.edu.cn; Nian Dong, PhD; Junjie Chen, PhD. Key Laboratory of Interventional Pulmonology of Zhejiang Province, Department of Pulmonary and Critical Care Medicine, The First Affiliated Hospital of Wenzhou Medical University, Shangcai Village, Ouhai District, Wenzhou 325000, China. Email: dongnian@wmu.edu.cn; chenjunjie@wmu.edu.cn.

Background: It has been proposed that repeated exposure of bronchial epithelial cells to atmospheric particulate matter (PM) could disrupt airway epithelial integrity and lead to epithelial-to-mesenchymal transition (EMT) and ultimately airway remodeling. The molecular mechanisms underlying PM-related bronchial epithelial EMT have not yet been elucidated. The aim of this research is to clarify the molecular mechanism of EMT upon PM exposure.

Methods: Using an *in vivo* mouse model of PM-induced airway inflammation and an *in vitro* model of PM-stimulated bronchial epithelial cells, we clarified the role of haptoglobin (HP) in PM-induced bronchial epithelial EMT. The expression of HP in lung tissues was evaluated by immunohistochemistry (IHC). Western blotting (WB) and immunofluorescence staining were used to analyze EMT-related protein expression and the relevant signaling pathways in the changes in lung tissues and bronchial epithelial cells upon PM exposure. HP small interfering RNA (siRNA) was used to implement the interference of endogenous HP.

Results: *In vivo* experiments showed elevated HP expression in the bronchial epithelium upon PM exposure. IHC and WB showed that E-cadherin expression was decreased, and vimentin expression was increased in bronchial epithelial cells. Moreover, WB results showed that the phosphorylation levels of signal transducer and activator of transcription 3 (STAT3) and extracellular regulated protein kinases (ERK) were elevated in the lung parenchymal tissue of mice. The results of *in vitro* molecular mechanism experiments showed that compared with those of the control group, the phosphorylation levels of STAT3 and ERK in the PM group increased progressively with higher concentrations of PM and longer stimulation durations. BEAS-2B cells were pretreated with stattic (STAT3 inhibitor) and/or U0126 (ERK inhibitor), and it was found that either stattic or U0126 inhibited PM-induced reduction of E-cadherin expression and elevation

of vimentin expression, and the inhibitory effect was most significant when both inhibitors were pretreated simultaneously. Through transfection of BEAS-2B cells with HP siRNA, WB results showed that HP siRNA partially reversed the PM-induced reduction in E-cadherin expression and elevation of vimentin expression, in addition to the reduction in the phosphorylation levels of the STAT3 and ERK.

Conclusions: HP is an important mediator of PM-induced EMT in bronchial epithelial cells and promotes PM-induced EMT in bronchial epithelial cells through activation of the STAT3 signaling pathway and the ERK signaling pathway. Inhibition of HP expression attenuates PM exposure-induced EMT in bronchial epithelial cells.

Keywords: Haptoglobin (HP); particulate matter (PM); epithelial-to-mesenchymal transition (EMT); bronchial epithelial cells

Submitted Nov 20, 2024. Accepted for publication Dec 21, 2024. Published online Dec 28, 2024.
doi: 10.21037/jtd-2024-2013
View this article at: https://dx.doi.org/10.21037/jtd-2024-2013

Introduction

With the intensification of industrialization and urbanization, atmospheric pollution has emerged as a global environmental issue. Particulate matter (PM) is a mixture of various noxious and carcinogenic substances and is regarded as the primary constituent of atmospheric pollutants (1,2). PM can be extensively deposited in the respiratory system due to its aerodynamic characteristics. Although the causal relationship between PM exposure and the morbidity of respiratory diseases has been confirmed, the pathophysiologic mechanism underlying PM exposure has not been elucidated (3,4). Further research into the critical molecules and pathophysiological processes underlying PM exposure is required to identify disease biomarkers and design innovative therapeutic strategies.

Haptoglobin (HP) is a hemoglobin-binding protein that is mainly synthesized and secreted by the liver (5). HP is involved in angiogenesis, immune response, antioxidant, and prostaglandin synthesis (6). Given its multifunctional effect, the lung has been recently recognized as the second site of origin for HP (7). The elevated expression of HP has been reported to be involved in the pathogenic process of respiratory diseases (7,8). HP expression is significantly elevated in most cases of rhinitis and asthma, suggesting its involvement in host defense responses to infection and inflammation. Airway hyperresponsiveness, a common feature in respiratory diseases, is associated with elevated levels of HP. Increased HP levels can elevate acute inflammatory molecules, exacerbating the disease. In chronic obstructive pulmonary disease (COPD), serum HP concentrations are significantly elevated and have been found to be more sensitive than C-reactive protein in reflecting the severity of the disease. Moreover, HP concentrations are positively correlated with the severity of COPD, indicating its potential role as a biomarker for monitoring disease progression (7). Additionally, studies have shown that HP can stimulate macrophages and alveolar epithelial cells to release cytokines such as interleukin-6 (IL-6), tumor necrosis factor-α (TNF-α), and monocyte chemoattractant protein-1 (MCP-1), which play important roles in airway inflammatory responses.

Highlight box

Key findings

- The haptoglobin (HP) and downstream signal transducer and activator of transcription 3 (STAT3)/extracellular regulated protein kinases (ERK) signaling pathways were found to play critical roles in epithelial-to-mesenchymal transition (EMT) of bronchial epithelial cells upon exposure to particulate matter (PM).

What is known and what is new?

- PM exposure could lead to the EMT process of bronchial epithelial cells which is a physiopathologic characteristic of airway remodeling, while the molecular mechanism of EMT remains to be elucidated.
- This study showed that the HP-STAT3/ERK signaling pathways are involved in process of EMT after PM exposure.

What is the implication, and what should change now?

- Our findings have broadened our understanding of the regulatory mechanism underlying the EMT process in bronchial epithelial cells upon PM exposure. HP might be a sensitive biomarker and therapeutic target for PM-related airway diseases.

Previously, we used gene profiling and proteomics methods to analyze biomarkers in acute exacerbations of COPD and found that HP was significantly increased at both the RNA and protein levels (8). Similarly, other studies have discovered the dysregulation of the CD163-HP axis in the airways of patients with COPD and association of HP phenotype with systemic inflammation and the severity of COPD (9,10). In buccal cancer cells, HP can elevate the expression of vimentin, a mesenchymal cell marker, and prompt epithelial-to-mesenchymal transition (EMT) (11).

EMT is a classical pathophysiological process in which polarized epithelial cells undergo various biochemical changes and eventually display mesenchymal cell traits (12). EMT is characterized by the downregulation of epithelial cell markers, such as E-cadherin, and the gradual acquisition of mesenchymal cell morphology and characteristics. This process includes an increase in the expression of mesenchymal cell markers, such as vimentin and fibronectin, which enhances the migration ability of epithelial cells. EMT is closely associated with tumor invasion and metastasis, and can serve as a biomarker for monitoring tumor formation and growth (13,14). Meanwhile, numerous studies have confirmed a close association between the EMT process and airway remodeling or fibrosis in various lung diseases, including COPD (15,16). Sohal *et al.* reported that cells in the basement membrane fissures of patients with COPD expressed S100A4, vimentin, and MMP9, indicating the presence of EMT in the airways of these patients, which is closely linked to airway remodeling (17). It has been proposed that the elevated incidence of lung cancer in patients with COPD stems from the stimulation of chronic inflammation in the airways, which leads to EMT. However, the precise mechanisms and key factors involved in the process of bronchial epithelial EMT, particularly when induced by PM exposure, remain unclear.

To date, the regulatory mechanism of HP and EMT in bronchial epithelial cells upon PM exposure has not been explored. We hypothesized that exposure to PM leads to elevated expression of HP in bronchial epithelial cells and that HP contributes to PM-induced EMT in bronchial epithelial cells, promoting airway remodeling. In this study, we investigated the expression of HP in PM-induced lung injury both *in vivo* and *in vitro*, along with the possible related underlying mechanisms. The findings indicate that HP plays a crucial role as a cytokine in regulating PM-induced EMT in bronchial epithelial cells via the signal transducer and activator of transcription 3 (STAT3) and extracellular regulated protein kinases (ERK) pathways. We present this article in accordance with the ARRIVE reporting checklist (available at https://jtd.amegroups.com/article/view/10.21037/jtd-2024-2013/rc).

Methods

Reagents and antibodies

PM 1649b was purchased from the National Institute of Standards and Technology (NIST; Gaithersburg, MD, USA). STAT3 inhibitor stattic and ERK inhibitor U0126 were obtained from Selleck Chemicals (Houston, TX, USA). Recombinant human HP (rhHP) was obtained from MedChemExpress (MCE; Monmouth Junction, NJ, USA). Antibodies of HP (Cat.#DF6467), E-cadherin (Cat.#BF0219), vimentin (Cat.#BF8006), and glyceraldehyde-3-phosphate dehydrogenase (GAPDH; Cat.#AF7021) were purchased from Affinity Biosciences (Cincinnati, OH, USA). Antibodies of p44/42 MAPK (ERK1/2) (Cat.#4695S), phospho-p44/42 MAPK (ERK1/2) (Cat.#4370T), STAT3 (Cat.#9139T), and phospho-STAT3 (Cat.#9145T) were purchased from Cell Signaling Technology (CST; Danvers, MA, USA). The enzyme-linked immunosorbent assay (ELISA) kits for mouse HP, mouse IL-6, mouse IL-8, human HP, human IL-6, and human IL-8 were obtained from Boyun Biotechnology (Shanghai, China).

Animals and cells

Male C57BL/6 mice (aged 6–8 weeks and weighing 20–25 g) were obtained from Beijing Vital River Laboratory Animal Technology Company (Beijing, China). These mice were housed in a standard, specific pathogen-free environment at The First Affiliated Hospital of Wenzhou Medical University, maintained at a temperature of 22–24 ℃, with unrestricted access to food and water. All experimental procedures conducted on animals underwent review and approval by the Animal Experiment Center Ethics Committee of Wenzhou Medical University (No. 2019-0462), and all animal surgeries were carried out strictly in accordance with both internationally recognized and institutional guidelines for the care and use of animals. A protocol was prepared before the study without registration.

Human bronchial epithelial cells (BEAS-2B) were obtained from the Chinese Academy of Sciences (Shanghai, China). The cells were cultured in Dulbecco's Modified

Eagle Media/Nutrient Mixture F-12 (DMEM/F-12; Gibco, Waltham, MA, USA) supplemented with 10% fetal bovine serum (FBS; Gibco) and 1% penicillin-streptomycin (Gibco) at 37 ℃ within the cell culture incubator with 5% CO_2.

Experimental design

For the *in vivo* experiments, mice were randomized into two groups (vehicle group and PM group; n=12 per group). After anesthesia with pentobarbital sodium, the PM group received 4 mg/kg PM suspension via intratracheal instillation for 2 consecutive days, while the vehicle group received an equal volume of sterile phosphate-buffered saline (PBS). The mice were euthanized 24 h after the last PM exposure. Bronchoalveolar lavage fluid (BALF), plasma, and lung tissues were collected for further analysis.

For the *in vitro* assays, the PM was suspended in sterile PBS to form a stock solution of 8 mg/mL, and BEAS-2B cells were treated with PM at 50, 100, 200, and 400 μg/mL for 24 h or 200 μg/mL for 3, 6, 12, and 24 h. Cells were treated with the STAT3 inhibitor (stattic; 2.5 μM) or ERK inhibitor (U0216; 5 μM) 1 h before PM treatment.

ELISA

BALF was collected via tracheal cannula with 1 mL of PBS instilled into the lungs. Plasma was obtained via orbital blood sampling. The levels of IL-6, IL-8, and HP in plasma and BALF of mice and BEAS-2B cell culture supernatant were measured using ELISA kits according to the manufacturer's protocols.

Hematoxylin and eosin (HE) staining and periodic acid-Schiff (PAS) staining

The harvested lung tissues were fixed in 4% paraformaldehyde for 24 h, and then the lung tissues were embedded in paraffin and accurately sectioned at 5 μm. For HE staining, the slides were deparaffinized and stained separately with HE for histological analysis. For PAS staining, after routine deparaffinization, the sections were oxidized in periodic acid, placed in Schiff's reagent, and then counterstained with hematoxylin. Three independent experienced pathologists, blinded to the group assignments, evaluated the pathologic images and scored the histologic analysis. The scheme for the lung inflammation scoring was as follows: (I) no inflammation; (II) occasional cuffing with inflammatory cells; (III) most bronchial vessels surrounded by a thin layer (1 to 5) of inflammatory cells; and (IV) most bronchi or vessels surrounded by a thick layer (>5) of inflammatory cells. The scheme for the pulmonary mucus scoring was as follows: (I) PAS+ circumferential goblet cells of total airway epithelial cells ≤5%; (II) PAS+ goblet cells 6–30%; (III) PAS+ goblet cells 31–60%; and (IV) PAS+ goblet cells >60%.

Immunohistochemical staining

Lung tissues were collected and fixed in 4% paraformaldehyde overnight at 4 ℃. The tissues were then embedded in paraffin and sectioned for immunohistochemical staining. Lung tissue sections were deparaffinized in xylene, rehydrated in alcohol, and incubated with primary antibody against HP (1:100 dilution) overnight at 4 ℃. The next day, after three washes in PBS, the sections were incubated with horseradish peroxidase (HRP)-conjugated secondary antibodies and then visualized with 3,3'-diaminobenzidine (DAB). Images were captured with a light microscope (Leica Microsystems, Wetzlar, Germany). The mean optical density was analyzed using ImageJ software (National Institutes of Health, Bethesda, MD, USA).

Immunofluorescence

Frozen lung tissue sections were fixed in methanol for 10 min and incubated overnight with antibodies against HP and epithelial cell adhesion molecule (EpCAM), followed by incubation with the corresponding secondary antibodies. 4,6'-diamidino-2-phenylindole (DAPI) was used for nuclear staining for 10 min. BEAS-2B cells were seeded on the coverslip in a 96-well plate. After PM exposure for 24 h, cells were washed in PBS and fixed in 4% paraformaldehyde for 30 min and then permeabilized with 0.1% Triton X-100 for 15 min and blocked with 5% bovine serum albumin (BSA) for 30 min at room temperature. The slides were incubated with the primary antibody HP (1:100 dilution) overnight at 4 ℃ and then incubated with Alexa Fluor 488 Conjugate secondary antibody (1:200 dilution). The nuclei were then stained with DAPI (Solarbio, Beijing, China) for 10 min at room temperature. Finally, the lung sections and cell slides were visualized under a fluorescence microscope (Leica Microsystems). The mean fluorescence intensity was analyzed using ImageJ software.

Cell Counting Kit-8 (CCK-8) cell viability assay

Cell viability assays were performed using CCK-8 assay. BEAS-2B cells were treated with PM at 50, 100, 200, and 400 μg/mL for 24 h or 200 μg/mL for 3, 6, 12, and 24 h. Subsequently, 10 μL of CCK-8 solution was added, and the cells were incubated at 37 ℃ for 2 h. The absorbance at 450 nm was measured using a microplate reader, and the viability percentage was adjusted using untreated cells.

Quantitative reverse transcriptase polymerase chain reaction (qRT-PCR)

The messenger RNA (mRNA) primers were synthesized by Sangon Biotech (Shanghai, China). Total RNA was isolated using TRIzol reagent (Invitrogen, Thermo Fisher Scientific, Waltham, MA, USA), and reverse transcription to first-strand complementary DNA (cDNA) was performed using a HiScript II Q RT SuperMix for qPCR Kit (Vazyme, Nanjing, China). Finally, qRT-PCR was performed using TB Green Premix ExTaqTM II (Takara Bio Inc., Kusatsu, Japan). The mRNA levels of HP were quantified by the ΔCt method, and GAPDH was used for normalization. Each sample was assayed in triplicate. The primer sequences were as follows:

GAPDH forward, 5'-AGAACATCATCCCTGCCTCTACTGG-3';

GAPDH reverse, 5'-CGCCTGCTTCACCACCTTCTTG-3';

HP forward, 5'-AGGCATTATGAAGGCAGCACAGTC-3';

HP reverse, 5'-CTCCAGGTCGTGAACGGCAAAG-3'.

Transfection with short interfering RNA

Control small interfering RNA (NC siRNA) and HP siRNA were designed and synthesized by GenePharma (Shanghai, China). BEAS-2B cells were grown overnight to approximately 40% confluence and transfected with human HP siRNA for 8 h using Lipofectamine 2000 (Invitrogen, Waltham, MA, USA) according to the manufacturer's protocol. The transfection medium was then replaced with a fresh medium, and the cells were cultured for an additional 48 h. BEAS-2B cells were then treated with 200 μg/mL PM for 24 h. The relevant sequences were as follows:

NC siRNA, 5'-UUCUCCGAACGUGUCACGUTT-3';

HP siRNA-1, 5'-GGAGUGUACACCUUAAACATT-3';

HP siRNA-2, 5'-CCAAUGCAUAAGGCAUUAUTT-3';

HP siRNA-3, 5'-GUAUGCGACUGGGAUCUUATT-3'.

Cell migration assay

Migration was evaluated by wound-healing and Transwell assays. For the wound-healing assay, BEAS-2B cells were seeded to at least 90% fusion in 12-well plates and then scratched with a micropipette. After one wash to remove the detached cells, cells were migrated into the wound area in the absence or presence of rhHP (10, 100, and 1000 ng/mL). The migrating cells were photographed at 0 and 24 h, and the scratch area was quantified using ImageJ software. The polycarbonate filter membrane (24-well insert, 8-μm pore size; Corning Costar, Corning, NY, USA) was used for the Transwell cell migration assay. Briefly, 200 μL of serum-free medium (5×10^5 cells) was added to the upper Transwell chamber, and 600 μL of medium containing 10% FBS was added to the lower chamber. After 48 h, the nonmigratory cells were removed, and the cells on the lower surface of the membrane were fixed in 4% paraformaldehyde for 30 min and stained with 1% crystal violet for 30 min. The number of stained cells in randomly selected fields was counted using ImageJ software.

Western blotting (WB)

Total proteins were lysed from homogenized lungs (n=3 per group) and cell samples with radio-immunoprecipitation assay lysis buffer (RIPA) containing 1% phenylmethanesulfonyl fluoride (PMSF) and phosphatase inhibitor. The protein concentration was determined using the Pierce BCA Protein Assay Kit (Thermo Fisher Scientific). Proteins were then separated via sodium dodecyl sulfate-polyacrylamide gel electrophoresis (SDS-PAGE) and transferred to polyvinylidene fluoride (PVDF) membranes. Nonspecific sites were blocked by incubating the membranes in protein-free rapid blocking buffer (EpiZyme, Shanghai, China) for 10 min at room temperature, followed by incubation with primary antibodies overnight at 4 ℃. These membranes were then washed three times with Tris-buffered saline with Tween (TBST) and probed with HRP-linked secondary antibodies for 1 h at room temperature, followed by three washes with TBST. Protein bands were visualized using the iBright CL1500 imaging system

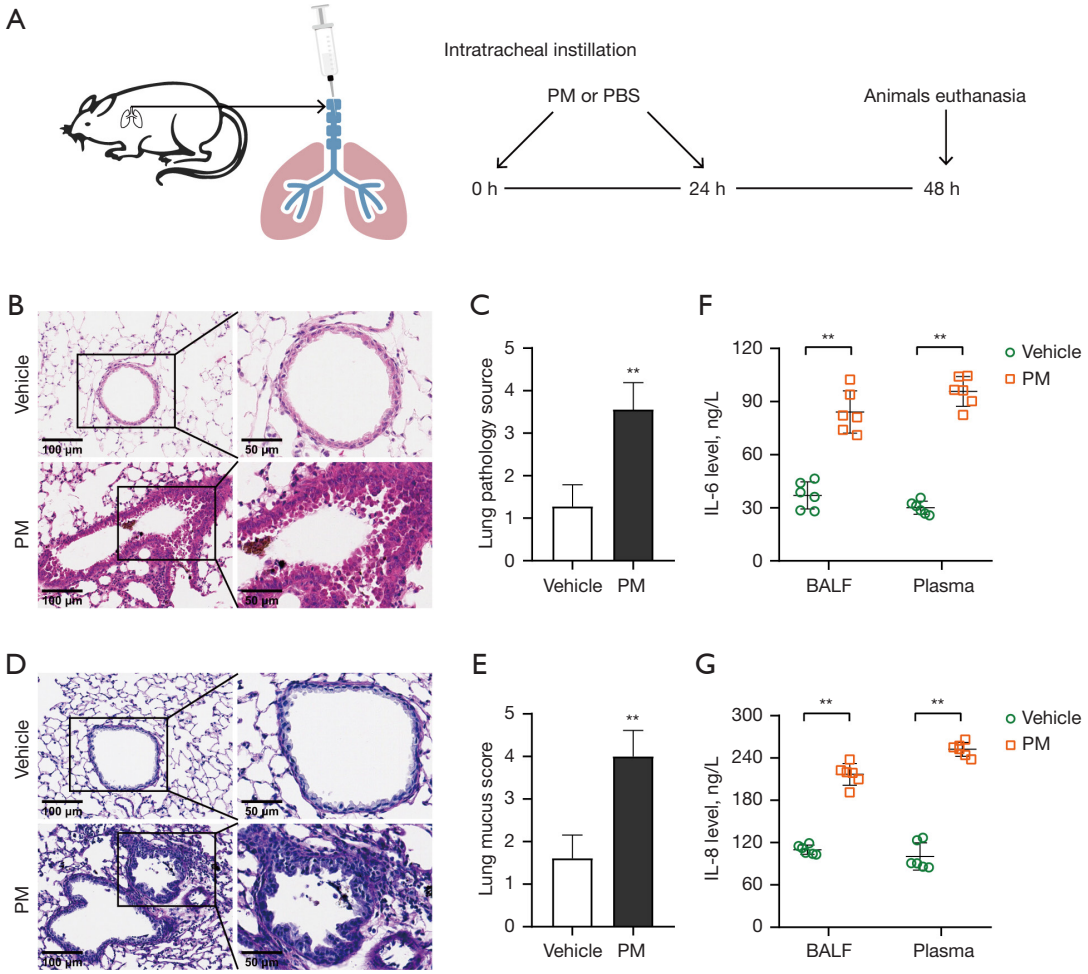

Figure 1 PM exposure induced airway inflammation in C57BL/6 mice. (A) The schematic diagram of the PM-induced airway inflammation model in mice. The C57BL/6 mice were intratracheally instilled with a dose of 4 mg/kg of PM for 2 consecutive days (n=12 per group). (B) Airway inflammation in mice was observed by HE staining (n=3). (C) Lung inflammation score for HE staining lung sections. (D) Airway mucus secretion in mice was observed by PAS staining (n=3). (E) Lung mucus score for PAS staining lung sections. (F,G) IL-6 and IL-8 levels in BALF and plasma were quantified by ELISA (n=6). The values are the mean ± SEM. **, P<0.01 *vs.* vehicle group. PM, particulate matter; BALF, bronchoalveolar lavage fluid; PBS, phosphate-buffered saline; IL, interleukin; HE, hematoxylin and eosin; PAS, periodic acid-Schiff; ELISA, enzyme-linked immunosorbent assay; SEM, standard error of measurement.

(Thermo Fisher Scientific). The intensity of protein bands was quantified using ImageJ software. GAPDH was used as the loading control.

Statistical analysis

All data are expressed as the mean ± standard error of measurement (SEM) and were analyzed using GraphPad Prism Version 8.0 (GraphPad Software, La Jolla, CA, USA). Statistical comparisons were made using the Student's *t*-test for two-group comparisons and one-way analysis of variance (ANOVA) comparisons of three or more groups. P<0.05 was considered to indicate a statistically significant difference.

Results

PM exposure induced airway inflammation in mice

We constructed a PM-induced mouse airway inflammation model as shown in *Figure 1A*. Morphologic lesions

and changes were observed in lung tissue sections via HE staining. There was no obvious inflammatory cell infiltration around the bronchus in the vehicle group, while the PM group showed PM particle deposition, peribronchial wall thickening, and inflammatory cell infiltration (*Figure 1B*). The inflammation score for the HE-stained lung sections was evaluated by three independent investigators. Consistent with the histopathologic analyses, the inflammation score was significantly higher in the PM exposure group than in the vehicle group (*Figure 1C*). The mucus secretion was observed in lung tissue sections by PAS staining. The results revealed that mucus secretion in the airways of PM-exposed mice was markedly higher than that in the vehicle group (*Figure 1D*). As with the inflammation score, the mucus score was also higher in the PM group (*Figure 1E*). The protein expression of inflammatory cytokines in BALF and plasma, IL-6 and IL-8, were quantified with ELISA. Compared with the vehicle group, PM exposure significantly upregulated the protein expression of IL-6 and IL-8 (*Figure 1F,1G*). These results suggest that PM could induce inflammation in mice.

PM exposure upregulated the expression of HP in vivo

To investigate the differential expression of HP in lung tissue of mice exposed to PM, a mouse model of PM-induced acute airway inflammation was established. Immunohistochemistry (IHC) staining showed that HP expression was significantly increased in PM-treated mice, especially in the bronchial epithelium of lung tissue (*Figure 2A*,*2B*). HP in BALF and serum was also tested via ELISA, and the results showed that PM-treated mice had a higher HP expression in BALF and serum than did the vehicle mice (*Figure 2C*,*2D*). WB of mice lung tissue showed upregulated expression of HP protein upon PM exposure (*Figure 2E*,*2F*). Immunofluorescence staining also showed that PM significantly increased the fluorescence intensity of HP (*Figure 2G*,*2H*). These results suggest that PM could significantly increase the expression of HP in the lung tissues of mice.

PM-induced EMT and activated STAT3/ERK signaling pathway in vivo

To investigate the impact of PM exposure on EMT in mice lungs, we conducted IHC to observe the expression of EMT-associated proteins (E-cadherin and vimentin). Our results revealed that in the PM group mice, there was a decrease in E-cadherin expression and an increase in vimentin expression compared to the vehicle group. This indicates the occurrence of EMT in the airways of mice exposed to PM (*Figure 3A-3D*). In addition, we analyzed the expression of the two proteins through WB and observed a decrease in E-cadherin and an increase in vimentin in the mice from the PM group (*Figure 3E-3G*). Notably, the STAT3/ERK signaling pathway was also activated in the PM group mice (*Figure 3H-3J*). These findings indicate that PM exposure could lead to airway EMT *in vivo*, along with the activation of the STAT3 and ERK signaling pathways.

PM-induced inflammation and EMT in cells and the effects of PM on cell viability and morphological changes

After treating BEAS-2B cells with varying PM concentrations or durations, we noted a gradual alteration in the cell phenotype following exposure to concentrations of PM exceeding 100 μg/mL for 24 h or 200 μg/mL for more than 12 h. Control cells displayed classic epithelial characteristics, while PM-treated cells transformed into a spindle-shaped mesenchymal phenotype (*Figure 4A*,*4B*). Subsequently, the dose- and time-dependent effects of PM on the viability of BEAS-2B cells were determined using CCK-8 assay. The cells were treated with varying concentrations of PM for different periods. The results indicated a gradual decrease in cell viability with increasing PM concentration, with the most significant effect noted at 24 h (*Figure 4C*,*4D*). IL-6 and IL-8 levels in the cell culture supernatant were quantified using ELISA. Objective analysis revealed a significant upregulation in the protein expression of IL-6 and IL-8 in the PM group compared to the control group (*Figure 4E,4F*). The WB analysis revealed a gradual decrease in the expression of E-cadherin in a dose- and time-dependent manner, whereas the expression of vimentin increased gradually. These findings suggest that the extent to which BEAS-2B cells undergo EMT intensifies with either an increase in PM concentration or a longer duration of stimulation (*Figure 4G-4L*). Based on these findings, a concentration of 200 μg/mL of PM for 24 h was selected for further experiments to clarify the *in vitro* effect of PM on BEAS-2B cells.

PM-induced HP expression in BEAS-2B cells

To validate the enhanced expression of HP *in vitro*, BEAS-2B cells underwent dose- and time-dependent stimulation with PM. The HP protein increased in BEAS-

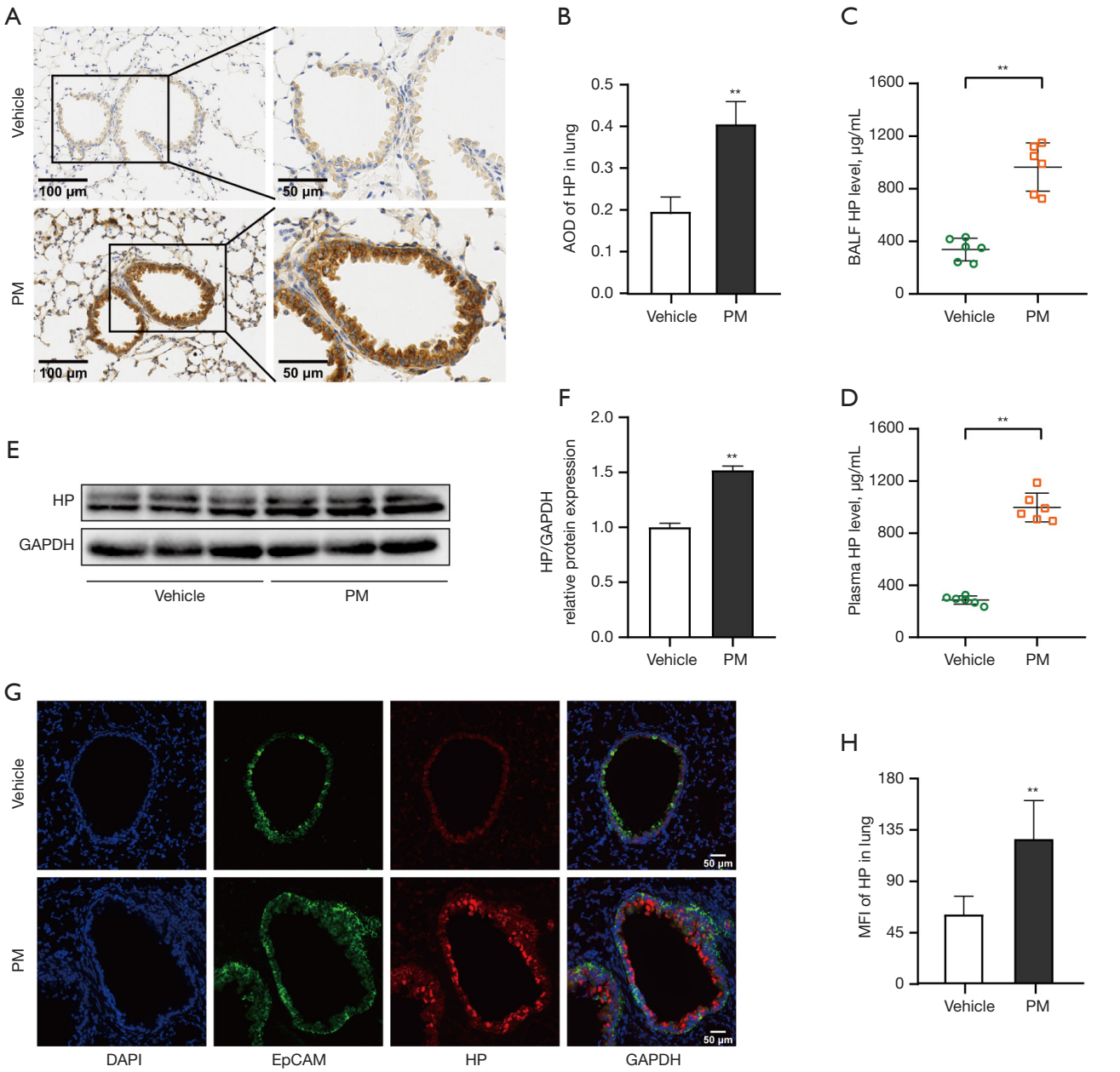

Figure 2 HP was upregulated upon PM exposure in mice. (A) The expression of HP in mouse bronchial epithelial cells was observed by immunohistochemical staining (n=3). (B) Average optical density of HP for immunohistochemical staining of lung sections. (C,D) HP levels in BALF and plasma were quantified by ELISA (n=6). (E) Western blotting analysis for HP protein expression in mouse lung tissues of each group (n=3). (F) The optical densities of protein bands. (G) Representative images of immunofluorescence staining of mouse bronchial epithelial cells. HP (red), EpCAM (green), and DAPI (blue) (n=3). (H) Mean fluorescence intensity of HP for immunofluorescence staining of lung sections. The values are the mean ± SEM. **, P<0.01 *vs.* vehicle group. PM, particulate matter; AOD, average optical density; HP, haptoglobin; BALF, bronchoalveolar lavage fluid; GAPDH, glyceraldehyde-3-phosphate dehydrogenase; DAPI, 4,6'-diamidino-2-phenylindole; EpCAM, epithelial cell adhesion molecule; MFI, mean fluorescence intensity; ELISA, enzyme-linked immunosorbent assay; SEM, standard error of measurement.

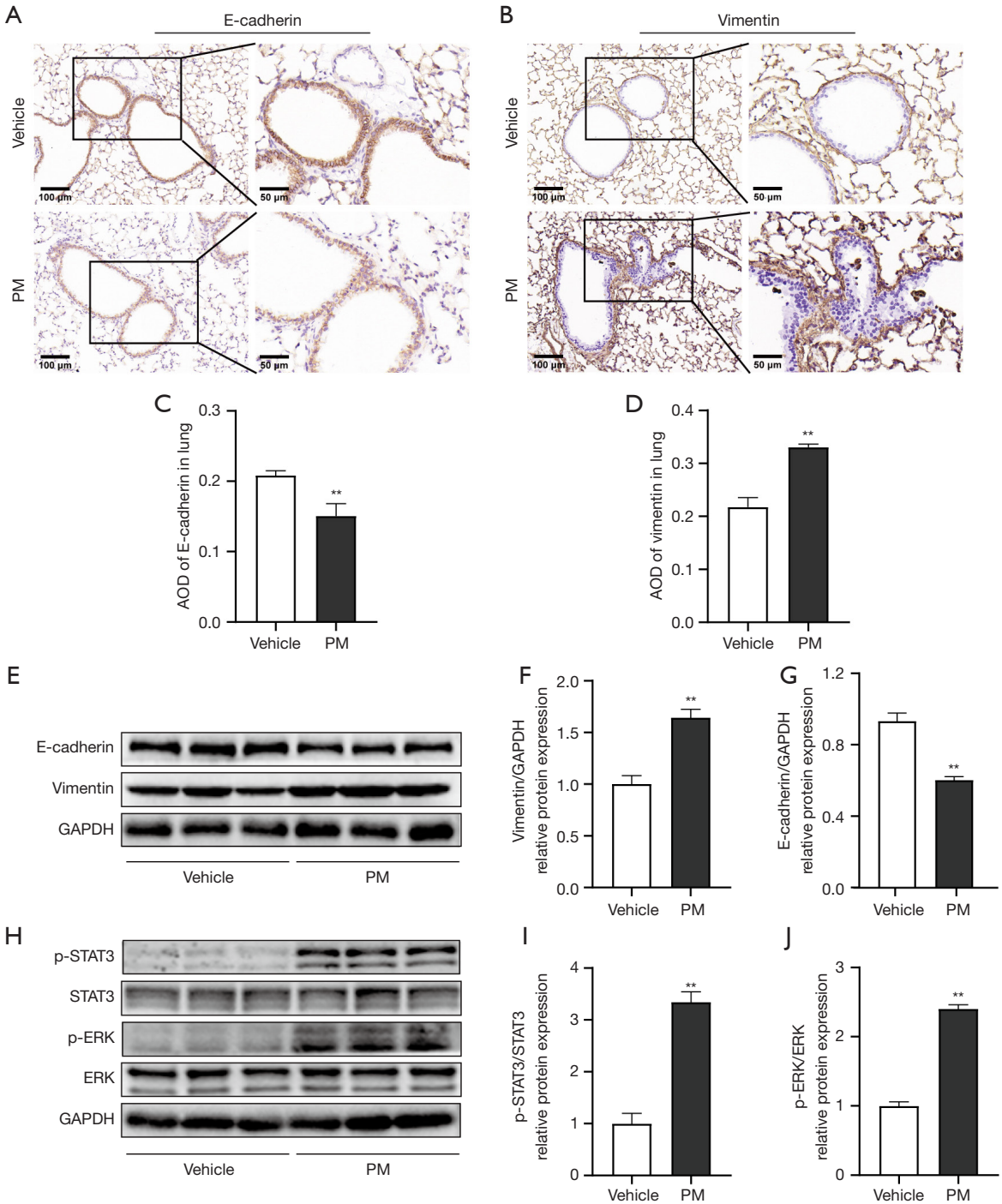

Figure 3 PM induced EMT in mice with activation of STAT3 and ERK pathways. (A,B) The expression of EMT-relevant E-cadherin and vimentin in murine bronchial epithelial cells was observed by immunohistochemical staining (n=3). (C,D) The average optical density of E-cadherin and vimentin for the immunohistochemical staining of lung sections. (E) Western blotting analysis for E-cadherin and vimentin protein expression in mouse lung tissues of each group (n=3). (F,G) The optical densities of protein bands. (H) Western blotting analysis for phosphorylation of STAT3 and ERK in mouse lung tissues of each group (n=3). (I,J) The optical densities of protein bands. The values are the mean ± SEM. **, P<0.01 *vs.* vehicle group. PM, particulate matter; AOD, average optical density; GAPDH, glyceraldehyde-3-phosphate dehydrogenase; EMT, epithelial-to-mesenchymal transition; SEM, standard error of measurement; STAT3, signal transducer and activator of transcription 3; ERK, extracellular regulated protein kinases.

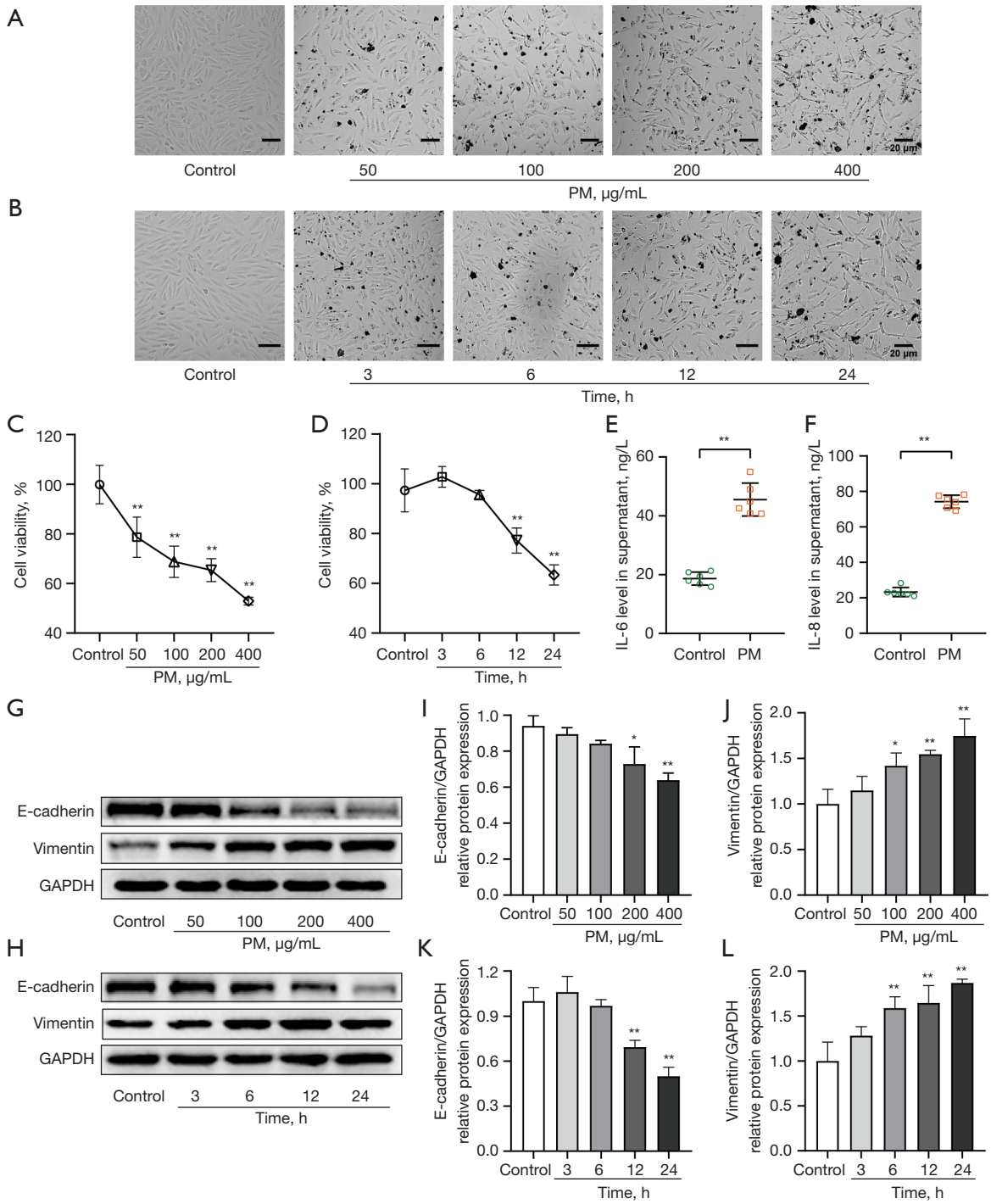

Figure 4 PM-induced inflammation and EMT in BEAS-2B cells and the effects of PM on cell viability and morphological changes. BEAS-2B cells were incubated with PM in a dose-dependent manner (0, 50, 100, 200, and 400 μg/mL) for 24 h or with 200 μg/mL of PM in a time-dependent manner (0, 3, 6, 12, and 24 h). (A,B) Representative images of cell morphological changes through optical microscope. (C,D) Cell viability was measured by CCK-8 assay. (E,F) IL-6 and IL-8 levels in the cell culture supernatant were quantified by ELISA (n=6). (G,H) Western blotting analysis of E-cadherin and vimentin protein expression in cells (n=3). (I-L) The optical densities of protein bands. The values are the mean ± SEM. *, P<0.05; **, P<0.01 *vs.* control group. Scale bar: 20 μm. PM, particulate matter; IL, interleukin; GAPDH, glyceraldehyde-3-phosphate dehydrogenase; EMT, epithelial-to-mesenchymal transition; CCK-8, Cell Counting Kit-8; ELISA, enzyme-linked immunosorbent assay; SEM, standard error of measurement.

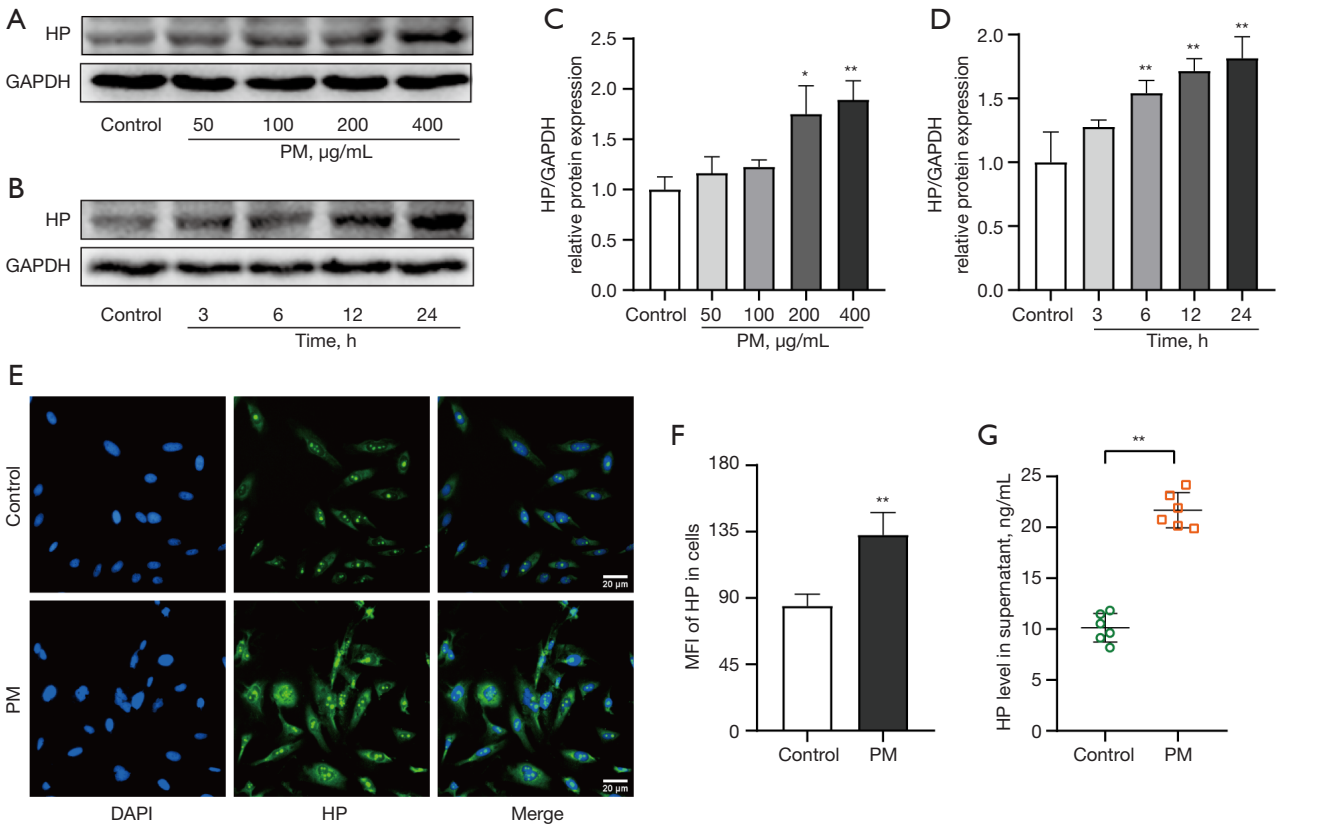

Figure 5 PM exposure induced HP expression in BEAS-2B cells. BEAS-2B cells were incubated with PM in a dose-dependent manner (0, 50, 100, 200, and 400 μg/mL) for 24 h or with 200 μg/mL of PM in a time-dependent manner (0, 3, 6, 12, and 24 h). (A,B) Western blotting analysis for HP protein expression in cells (n=3). (C,D) The optical densities of protein bands. (E) BEAS-2B cells were treated with 200 μg/mL PM for 24 h. Immunofluorescence staining was used to assess HP levels within the cells. (F) Mean fluorescence intensity of HP for immunofluorescence staining in cells. (G) HP content in cell culture supernatant was quantified by ELISA. (n=6). The values are the mean ± SEM. *, P<0.05; **, P<0.01 *vs.* control group. HP, haptoglobin; GAPDH, glyceraldehyde-3-phosphate dehydrogenase; PM, particulate matter; DAPI, 4,6'-diamidino-2-phenylindole; MFI, mean fluorescence intensity; ELISA, enzyme-linked immunosorbent assay; SEM, standard error of measurement.

2B cells treated with PM in a dose- and time-dependent manner (*Figure 5A-5D*). Moreover, when BEAS-2B cells were stimulated with 200 μg/mL of PM for 24 h, the immunofluorescent staining showed elevated HP levels in the PM-treated cells (*Figure 5E,5F*). HP expression in cell culture supernatant was measured using ELISA, and the results indicated that cells treated with PM had higher HP expression compared to the control group (*Figure 5G*). These findings suggest that PM notably enhances HP expression in BEAS-2B cells.

The role of STAT3 and ERK pathways in PM-induced EMT

To determine the activation of the signaling pathway in BEAS-2B cells treated with PM, the cells were exposed to various doses of PM and for different durations. The WB results indicated that PM induce the activation of the STAT3 and ERK signaling pathways in a dose- and time-dependent manner, respectively (*Figure 6A-6F*). Subsequently, BEAS-2B cells were treated with stattic and/or U0126 1 h before PM stimulation. Stattic and/or U0126

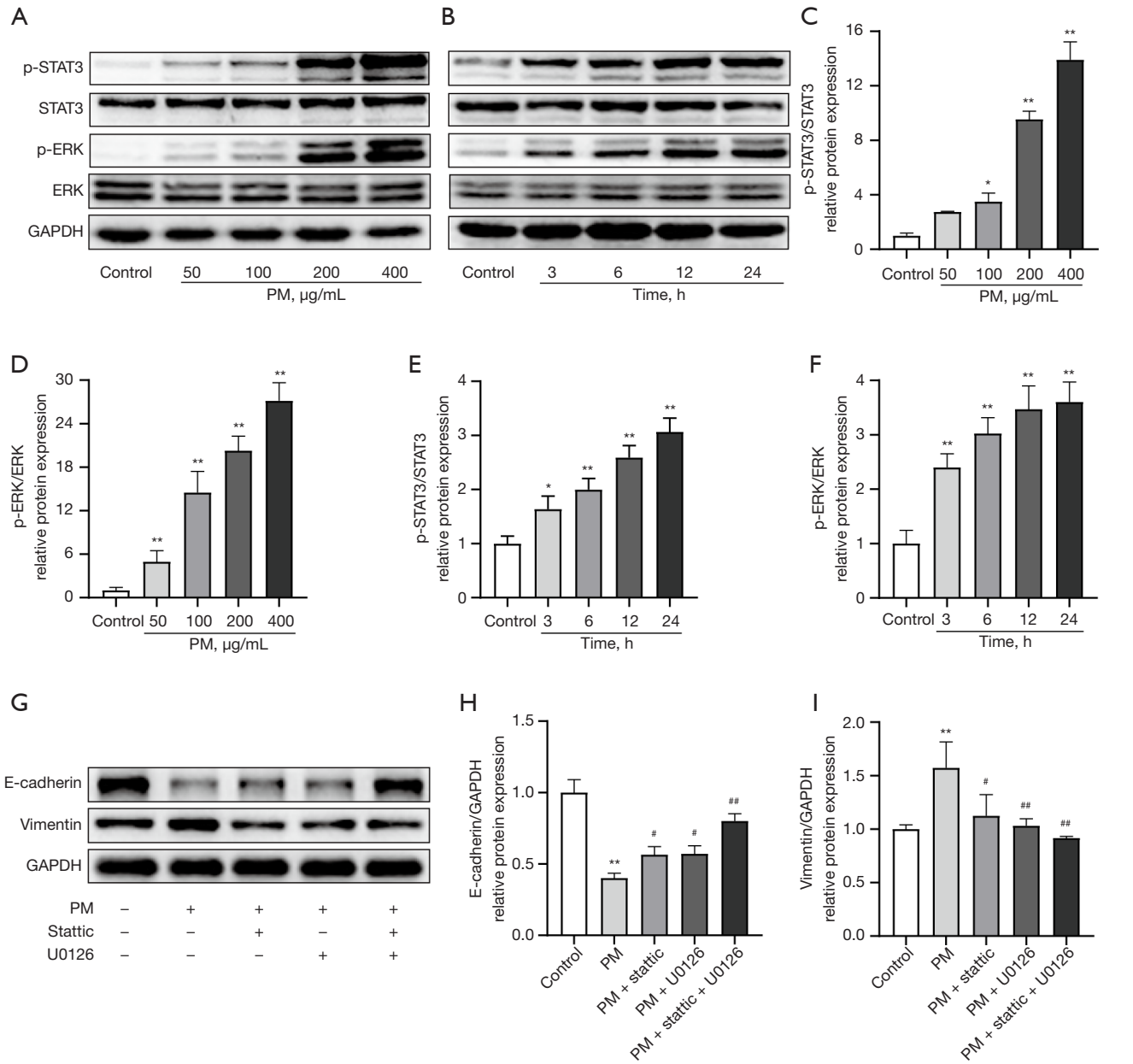

Figure 6 PM activated STAT3 and ERK pathways in BEAS-2B cells. The cells were exposed to PM in a dose-dependent manner (0, 50, 100, 200, and 400 μg/mL) for 24 h or with 200 μg/mL of PM in a time-dependent manner (0, 3, 6, 12, and 24 h). (A,B) Western blotting analysis was conducted to detect the activation of STAT3 and ERK signaling pathways in cells (n=3). (C-F) The optical densities of protein bands. (G) BEAS-2B cells were treated with stattic (2.5 μM) and/or U0126 (5 μM), followed by 24-h incubation with 200 μg/mL of PM. E-cadherin and vimentin protein expression in cells were analyzed using Western blotting (n=3). (H,I) The optical densities of protein bands. The values are the mean ± SEM. *, P<0.05; **, P<0.01 *vs.* control group. $^{\#}$, P<0.05; $^{\#\#}$, P<0.01 *vs.* control group. Stattic, STAT3 inhibitor; U0126, ERK inhibitor; PM, particulate matter; GAPDH, glyceraldehyde-3-phosphate dehydrogenase; SEM, standard error of measurement; STAT3, signal transducer and activator of transcription 3; ERK, extracellular regulated protein kinases.

could block PM-induced EMT, and the inhibitory effect was most significant in BEAS-2B cells pretreated with both inhibitors (*Figure 6G-6I*). These findings demonstrate that PM could induce EMT in BEAS-2B cells through the STAT3 and ERK signaling pathways.

HP siRNA attenuated PM-induced EMT and STAT3/ERK pathway activation in cells

To investigate the impact of HP knockout on PM-induced EMT, BEAS-2B cells underwent HP siRNA transfection. Three distinct HP siRNA constructs were designed, and the first one was chosen based on the reduced level of HP mRNA in each group compared to the control group, as determined by qRT-PCR (*Figure 7A*). Following HP siRNA transfection, BEAS-2B cells were treated with 200 μg/mL of PM for 24 h. We observed that HP siRNA inhibited both PM-induced EMT and the activation of STAT3 and ERK signaling pathways (*Figure 7B-7F*). The results of the migration assay indicated a significant increase in cellular migration following a 24 h treatment of PM. Conversely, when HP was knocked out before PM treatment, the migration ability of the cells decreased (*Figure 7G,7H*). These findings suggest that HP potentiates PM-induced EMT and activates the STAT3 and ERK signaling pathways in BEAS-2B cells.

rbHP enhanced cell migration and promoted PM-induced EMT and STAT3/ERK pathway activation

To verify the impact of HP on PM-induced EMT, BEAS-2B cells were administered rhHP 1 h before exposure to PM. A wound healing assay was performed to measure cell migration in response to varying concentrations of HP. The results indicated that BEAS-2B cells exhibit increased migratory properties following treatment with dose-dependent rhHP (*Figure 8A,8B*). We subsequently administered 100 ng/mL of rhHP 1 h before PM treatment. WB analyses demonstrated that exogenous HP facilitates PM-induced EMT while activating the STAT3 and ERK signaling pathways (*Figure 8C-8G*). These results provided additional evidence that exogenous HP could enhance PM-induced EMT and signaling activation in BEAS-2B cells.

Discussion

Increasing air pollution is a key factor contributing to the growing incidence of airway diseases, with PM being one of the important components of air pollutants. Bronchial epithelial cells are the primary barrier of the respiratory system against air pollutants, and PM can be widely deposited in the bronchial epithelium with respiratory airflow. The inflammatory damage and abnormal repair of the airway epithelium caused by PM play a crucial role in the onset and progression of airway diseases (18). Epithelial cells can be transformed into stromal cells through EMT and then obtain strong migration ability and extracellular matrix secretion ability to facilitate cell migration and tissue regeneration. Airway epithelial EMT is closely related to the inflammatory damage and remodeling of the airway epithelium (19,20). The airway epithelial EMT is closely related to the occurrence and development of airway disease, but the underlying molecular mechanisms remain unclear. Examining the repair of airway epithelial inflammatory damage in the initial stage of airway diseases, identifying the key inflammatory mediators, and investigating the role and mechanism of PM in airway epithelial EMT are of great significance for the diagnosis and treatment of these diseases.

HP is considered a potential regulatory mediator of inflammation. Previous animal experiments have demonstrated that PM exposure can lead to increased serum HP secretion levels, which is accompanied by the expression of HP derived from airway epithelial cells, suggesting that HP may be involved in the inflammatory response and damage-repair process of airway epithelium (21). Previous studies suggest that PM exposure can cause EMT in airway epithelium (22-24). Similarly, it has been reported that HP can promote the expression of the stromal cell marker vimentin in oral cancer cells, with the potential capability of induction of the EMT process (11). Currently, there are no similar reports confirming whether PM can upregulate HP expression and subsequently induce EMT in bronchial epithelial cells. The specific mechanisms by which PM may influence this process remain unclear. Therefore, we combined *in vivo* animal experiments and *in vitro* cell experiments to clarify the role of HP in the induction of EMT in bronchial epithelial cells via PM and to examine the potentially related signal transduction mechanisms.

In this study, we developed an animal model of short-term PM exposure. Our findings indicate that PM can be extensively deposited in the lungs, particularly within the bronchi, which was associated with thickening of the bronchial wall, infiltration of inflammatory cells, increased mucus secretion, and a significantly increased level of HP

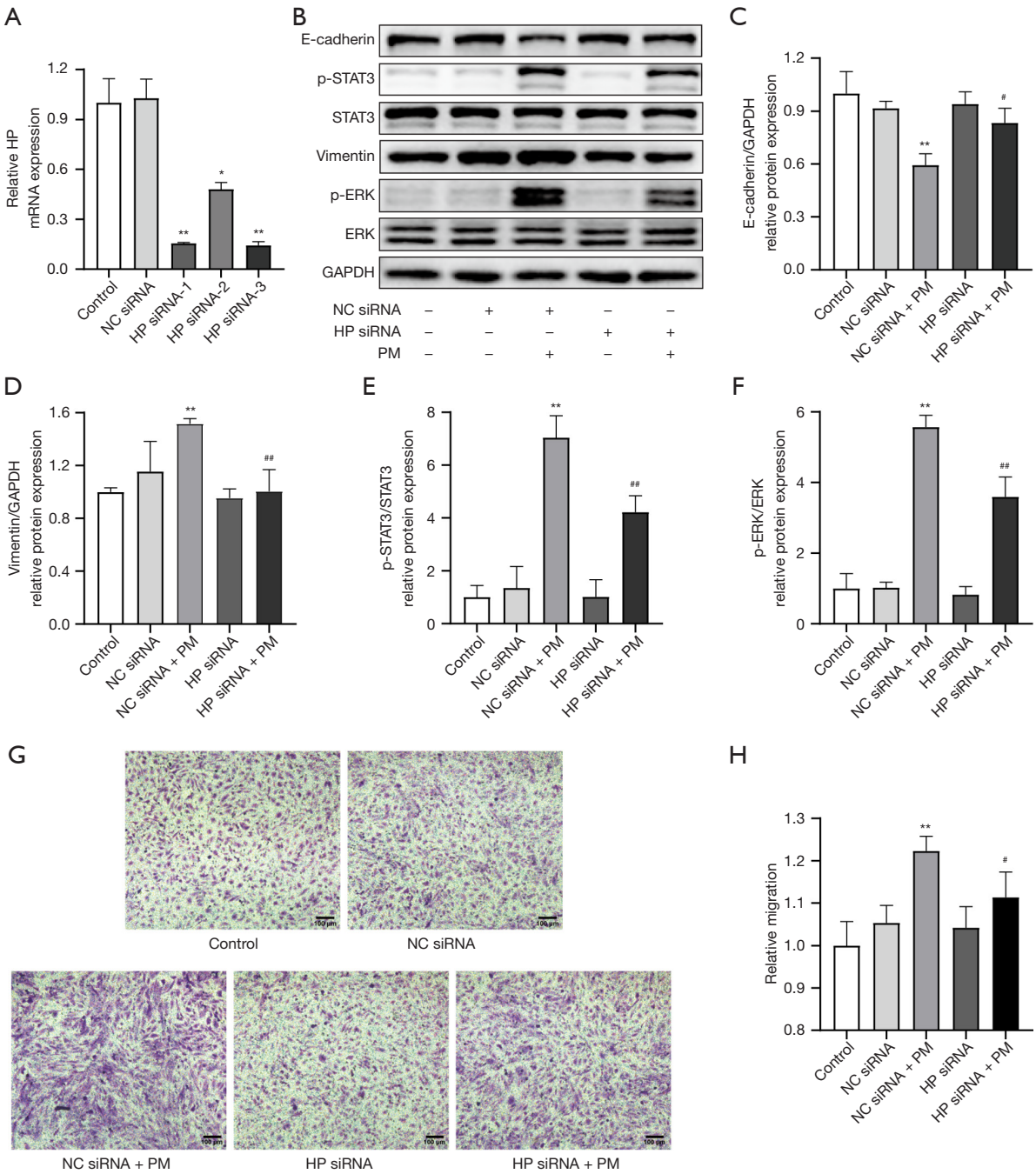

Figure 7 HP siRNA inhibited PM-induced EMT and STAT3/ERK pathway activation in BEAS-2B cells. BEAS-2B cells were transfected with HP siRNA and then incubated with 200 μg/mL of PM for 24 h. (A) The most effective HP siRNA was determined by qRT-PCR. (B) Western blotting analysis for the protein expression of E-cadherin and vimentin and the activation of the STAT3/ERK signaling pathway in cells. (n=3). (C-F) The optical densities of protein bands. (G) The effect of PM on the migration of cells was observed via Transwell assay through crystal violet. (H) Quantification of the Transwell migration assay. The values are the mean ± SEM. *, P<0.05; **, P<0.01 *vs.* control group. #, P<0.05; ##, P<0.01 *vs.* control group. HP, haptoglobin; GAPDH, glyceraldehyde-3-phosphate dehydrogenase; NC, negative control; PM, particulate matter; PCR, polymerase chain reaction; SEM, standard error of measurement; STAT3, signal transducer and activator of transcription 3; ERK, extracellular regulated protein kinases; siRNA, small interfering RNA; qRT-PCR, quantitative reverse transcriptase polymerase chain reaction.

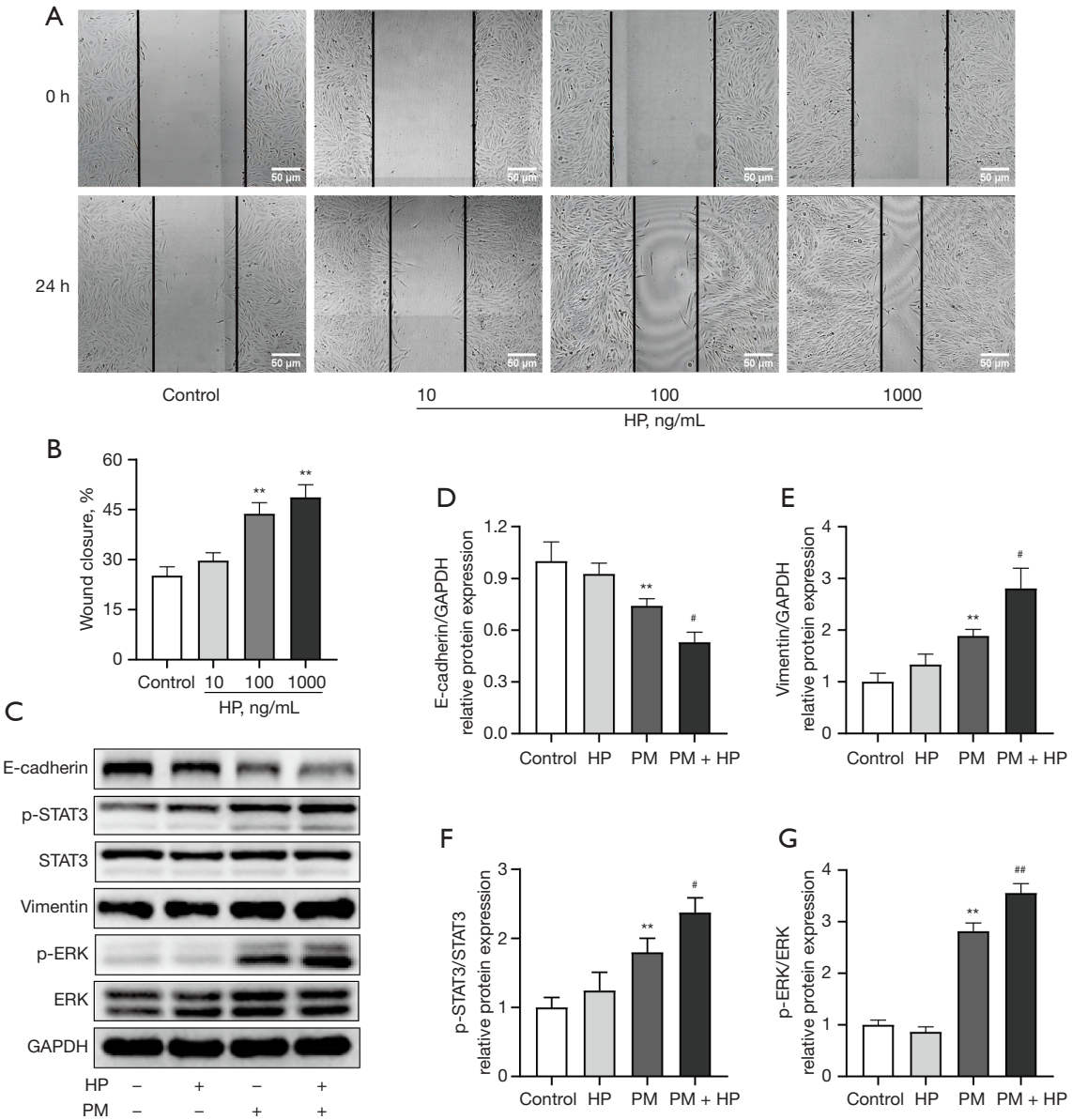

Figure 8 Exogenous HP increased the migration ability of BEAS-2B cells and facilitated PM-induced EMT and activation of the STAT3/ERK pathway. (A) BEAS-2B cells were treated with varying doses (0, 10, 100, and 1,000 ng/mL) of rhHP for 24 h. Representative images of cell migration were observed through wound-healing assay. (B) Quantification of the wound healing assay. (C) BEAS-2B cells were treated with 100 ng/mL rhHP and 200 μg/mL PM for 24 h. The protein expression of E-cadherin and vimentin and activation of the STAT3/ERK signaling pathway in cells were analyzed using Western blotting (n=3). (D-G) The optical densities of protein bands. The values are the mean ± SEM. **, P<0.01 *vs.* control group. #, P<0.05; ##, P<0.01 *vs.* control group. HP, haptoglobin; GAPDH, glyceraldehyde-3-phosphate dehydrogenase; PM, particulate matter; EMT, epithelial-to-mesenchymal transition; rhHP, recombinant human HP; SEM, standard error of measurement; STAT3, signal transducer and activator of transcription 3; ERK, extracellular regulated protein kinases.

secretion in BALF and plasma. In this study, *in vivo* animal experiments indicated that PM exposure downregulates E-cadherin and upregulates stromal marker vimentin, indicating that PM exposure can induce EMT in airway epithelial cells. *In vitro* experiments similarly demonstrated that the degree of EMT in bronchial epithelial cells intensifies with increasing concentration of PM or prolonged exposure times. This process is accompanied by corresponding expression changes of HP. Thevenot *et al.* also found that when BEAS-2B bronchial epithelial cells were exposed to synthetic ultrafine particles (UFPs), they underwent the process of EMT, as manifest by the reduced epithelial cell marker E-cadherin and mesenchymal cell marker α-SMA (25). EMT finger-polarized epithelial cells undergo multiple biochemical alterations that ultimately exhibit stromal cell properties. EMT is characterized by the downregulation of the epithelial cell marker E-cadherin, with epithelial cells progressively acquire the morphology and characteristics of stromal cells. EMT is mainly involved in three major pathophysiological processes: embryonic development and organ formation, tumorigenesis and metastasis, and tissue damage and repair (16,26). The EMT of bronchial epithelial cells is closely related to the inflammatory damage and repair of airway epithelial cells. However, repeated stimulation by PM can easily cause uncontrolled airway epithelial EMT, leading to abnormal repair and subsequent airway remodeling (27,28). Recently, it was shown that the pathways causing inflammation and oxidative stress from PM exposure are also involved in the induction of EMT (29). However, the key mediators related to the initiation of PM-induced EMT in the airway epithelium have not yet been elucidated.

HP is an acute time-phase protein that can be expressed in type II alveolar epithelial cells, alveolar macrophages, and bronchial epithelia. Many previous studies have shown that the expression level of HP is significantly increased in various inflammatory environments, commonly in conditions such as inflammation, tissue injury, infection, trauma, and various malignancies (30,31). Pulmonary HP is considered part of the pulmonary superactive component. Its expression level is elevated during inflammation and infection, where it plays a role in immune regulation. This makes it a part of the pulmonary self-protection mechanisms (32,33). In this study, *in vivo* animal experiments indicated that PM-induced EMT in the development of airway epithelium was accompanied by the elevated expression of HP. Through *in vitro* cell experiments, we found that PM exposure led to elevated expression of HP in airway epithelial cells, accompanied by a decrease in E-cadherin expression and an increase in vimentin expression. Moreover, this study found that interference of bronchial epithelial HP expression by siRNA blocked PM-induced bronchial epithelial EMT, and the rhHP protein could promote PM-induced airway epithelial EMT, suggesting that HP acts as an important mediator to promote PM-induced bronchial epithelial EMT. Though the regulatory effect of HP on EMT is investigated, the multifunctional effect of HP in bronchial epithelial cell cycle progression and apoptosis remains to be elucidated.

Recently, related studies have found that PM exposure may activate signaling pathways such as NF-κB, MAPK, and TGF-β (29,34). Meanwhile, related studies have reported that the abovementioned signaling pathways are involved in the PM-induced EMT process. However, the specific mechanism still needs to be elucidated. Our study aimed to further elucidate the mechanism by which HP promotes PM-induced EMT in bronchial epithelial cells. We discovered that PM exposure led to elevated expression of EMT and HP, alongside the activation of STAT3 signaling and ERK signaling pathway in these cells. STAT3 is an important member of the STAT family and is involved in the regulation of several important biological functions, including cell proliferation and differentiation, angiogenesis, and immune response. The STAT3 signaling pathway has been demonstrated to play an important role in the EMT process in pancreatic cancer by regulating Snail gene expression (35). The IL-6-STAT3-Fra-1 signaling axis can be involved in the EMT and metastasis of colorectal cancer by inducing Snail, Slug, ZEB 1, MMP-2, and MMP-9 (36). Meanwhile, our findings indicated that the inflammation caused by PM can activate IL-6, which in turn can induce EMT by regulating the JAK/STAT3 signaling pathway (37). As a member of the MAPK family, the ERK functions in the ERK/MAPK signaling pathway include the regulation of biological processes such as development, apoptosis, autophagy, tumorigenesis, and inflammation. The ERK/MAPK pathway is involved in the progression of EMT in different pulmonary diseases (38-40). This study found that blockade of the signaling pathway by specific STAT3 and ERK inhibitors could reverse PM-induced airway epithelial EMT. The activation of STAT3 and ERK signaling decreased after HP interference in airway epithelial cells, which subsequently inhibited PM-induced of EMT. Conversely, rhHP protein was found to promote PM-induced EMT by enhancing the activation of both the STAT3 and ERK signaling pathways in these

cells. Additionally, PM exposure was shown to induce EMT in bronchial epithelial cells with elevated HP expression. Thus, HP appears to facilitate PM-induced EMT in airway epithelial cells by activating the STAT3 and ERK signaling pathways.

This study had certain limitations that should be addressed. First, constructing the animal model of PM-induced airway inflammation, the method of PM airway infusion may have altered the aerodynamic properties of PM. Moreover, the constituents of PM include sulfates, nitrates, ammonium, acids, heavy metals, polycyclic aromatic hydrocarbons and so on. As for the potential EMT mediators of PM, it remains to be further elucidated and would be the direction of further research. Second, the study primarily concentrated on the repair of airway epithelium following inflammatory damage. Besides the bronchial epithelial cells, the innate immunocyte such as macrophages should be paid attention to as well. The use of an animal model with short-term PM exposure primarily highlighted the repair of inflammatory damage to the airway epithelium, which may not fully represent the chronic effects of PM exposure. Introducing an animal model of chronic, continuous PM exposure would allow for a dynamic observation of the entire process from airway inflammation repair to structural remodeling. And long-term PM exposure would allow us to explore the effect of HP on fibrogenesis, which would be our next research direction. This approach would enable a more comprehensive characterization of the role of HP in these processes. Finally, the signaling pathways involved are complex, including STAT3, EKR, PI3K, Nrf2 and so on. While this study focused on the STAT3 and ERK signaling pathways based on a literature review and preliminary pre-experiments, utilizing gene sequencing to screen for related signaling pathways could enhance the accuracy and scope of the study's exploration of molecular mechanisms. This could provide a more detailed understanding of the pathways involved in PM-induced EMT and the role of HP in airway epithelial cells.

Conclusions

In conclusion, this study elucidated that PM exposure leads to the expression and secretion of HP in bronchial epithelial cells. It was demonstrated that PM can induce EMT in these cells, with the extent of EMT being dependent on PM concentration and the duration of exposure. The study identified the STAT3 and ERK signaling pathways as key mediators in the PM-induced EMT processes within the bronchial epithelium. HP emerged as a crucial mediator of PM-induced EMT; by activating the STAT3 and ERK pathways. These findings may offer novel targets for the prevention and treatment of chronic airway diseases.

Acknowledgments

Funding: The work was supported by the Zhejiang Provincial Natural Science Foundation (No. LQ20H010002), Zhejiang Provincial Science Technology Department Foundation (No. 2024KY145), and Zhejiang Province Disease Prevention and Control Foundation (No. 2025JK232).

Footnote

Reporting Checklist: The authors have completed the ARRIVE reporting checklist. Available at https://jtd.amegroups.com/article/view/10.21037/jtd-2024-2013/rc

Data Sharing Statement: Available at https://jtd.amegroups.com/article/view/10.21037/jtd-2024-2013/dss

Peer Review File: Available at https://jtd.amegroups.com/article/view/10.21037/jtd-2024-2013/prf

Conflicts of Interest: All authors have completed the ICMJE uniform disclosure form (available at https://jtd.amegroups.com/article/view/10.21037/jtd-2024-2013/coif). The authors have no conflicts of interest to declare.

Ethical Statement: The authors are accountable for all aspects of the work in ensuring that questions related to the accuracy or integrity of any part of the work are appropriately investigated and resolved. All protocols for animal experiments were approved by the Animal Experiment Center Ethics Committee of Wenzhou Medical University (No. 2019-0462), and all animal surgeries were carried out strictly in accordance with both internationally recognized and institutional guidelines for the care and use of animals.

References

1. Abelenda-Alonso G, Satorra P, Marí-Dell'Olmo M, et al. Short-Term Exposure to Ambient Air Pollution and Antimicrobial Use for Acute Respiratory Symptoms. JAMA Netw Open 2024;7:e2432245.
2. Ma J, Chiu YF, Kao CC, et al. Fine particulate matter manipulates immune response to exacerbate microbial pathogenesis in the respiratory tract. Eur Respir Rev 2024;33:230259.
3. Ning Z, Ma Y, He S, et al. High altitude air pollution and respiratory disease: Evaluating compounded exposure events and interactions. Ecotoxicol Environ Saf 2024;285:117046.
4. Yang T, Chen R, Gu X, et al. Association of fine particulate matter air pollution and its constituents with lung function: The China Pulmonary Health study. Environ Int 2021;156:106707.
5. Naryzhny SN, Legina OK. Haptoglobin as a biomarker. Biomed Khim 2021;67:105-18.
6. Chrostek L, Gan K, Kazberuk M, et al. Acute-phase proteins as indicators of disease severity and mortality in COVID-19 patients. Sci Rep 2024;14:20360.
7. Arellano-Orden E, Calero-Acuña C, Cordero JA, et al. Specific networks of plasma acute phase reactants are associated with the severity of chronic obstructive pulmonary disease: a case-control study. Int J Med Sci 2017;14:67-74.
8. Shi L, Zhu B, Xu M, et al. Selection of AECOPD-specific immunomodulatory biomarkers by integrating genomics and proteomics with clinical informatics. Cell Biol Toxicol 2018;34:109-23.
9. Lee PL, Lee KY, Cheng TM, et al. Relationships of Haptoglobin Phenotypes with Systemic Inflammation and the Severity of Chronic Obstructive Pulmonary Disease. Sci Rep 2019;9:189.
10. Higham A, Baker JM, Jackson N, et al. Dysregulation of the CD163-Haptoglobin Axis in the Airways of COPD Patients. Cells 2021;11:2.
11. Lee CC, Ho HC, Chien SH, et al. Association of acute phase protein-haptoglobin, and epithelial-mesenchymal transition in buccal cancer: a preliminary report. Clin Chem Lab Med 2013;51:429-37.
12. Wang X, Xue X, Pang M, et al. Epithelial-mesenchymal plasticity in cancer: signaling pathways and therapeutic targets. MedComm (2020) 2024;5:e659.
13. Aftabi S, Barzegar Behrooz A, Cordani M, et al. Therapeutic targeting of TGF-β in lung cancer. FEBS J 2024. [Epub ahead of print]. doi: 10.1111/febs.17234.
14. Hu D, Zhao T, Xu C, et al. Epigenetic Modifiers in Cancer Metastasis. Biomolecules 2024;14:916.
15. He H, Ji X, Cao L, et al. Medicine Targeting Epithelial-Mesenchymal Transition to Treat Airway Remodeling and Pulmonary Fibrosis Progression. Can Respir J 2023;2023:3291957.
16. Mottais A, Riberi L, Falco A, et al. Epithelial-Mesenchymal Transition Mechanisms in Chronic Airway Diseases: A Common Process to Target? Int J Mol Sci 2023;24:12412.
17. Sohal SS. Epithelial and endothelial cell plasticity in chronic obstructive pulmonary disease (COPD). Respir Investig 2017;55:104-13.
18. Zeng Y, Bai X, Zhu G, et al. m(6)A-mediated HDAC9 upregulation promotes particulate matter-induced airway inflammation via epigenetic control of DUSP9-MAPK axis and acts as an inhaled nanotherapeutic target. J Hazard Mater 2024;477:135093.
19. Lu W, Eapen MS, Hardikar A, et al. Epithelial-mesenchymal transition changes in nonsmall cell lung cancer patients with early COPD. ERJ Open Res 2023.
20. Wu Z, Chen X, Wu S, et al. Transcriptome analysis reveals the impact of NETs activation on airway epithelial cell EMT and inflammation in bronchiolitis obliterans. Sci Rep 2023;13:19226.
21. Pace A, Villamediana P, Rezamand P, et al. Effects of wildfire smoke PM2.5 on indicators of inflammation, health, and metabolism of preweaned Holstein heifers. J Anim Sci 2023;101:skad246.
22. Chi Y, Huang Q, Lin Y, et al. Epithelial-mesenchymal transition effect of fine particulate matter from the Yangtze River Delta region in China on human bronchial epithelial cells. J Environ Sci (China) 2018;66:155-64.
23. Lin Q, Chen X, Huo T, et al. PM(2.5) dust induces autophagy and epithelial-mesenchymal transition in human bronchial epithelial 16HBE cells. Xi Bao Yu Fen Zi Mian Yi Xue Za Zhi 2022;38:328-32.
24. Yu SL, Koo H, Kang Y, et al. Exosomal miR-196b secreted from bronchial epithelial cells chronically exposed to low-dose PM(2.5) promotes invasiveness of adjacent and lung cancer cells. Toxicol Lett 2024;399:9-18.
25. Thevenot PT, Saravia J, Jin N, et al. Radical-containing

ultrafine particulate matter initiates epithelial-to-mesenchymal transitions in airway epithelial cells. Am J Respir Cell Mol Biol 2013;48:188-97.
26. Rubio K, Castillo-Negrete R, Barreto G. Non-coding RNAs and nuclear architecture during epithelial-mesenchymal transition in lung cancer and idiopathic pulmonary fibrosis. Cell Signal 2020;70:109593.
27. Hou W, Hu S, Li C, et al. Cigarette Smoke Induced Lung Barrier Dysfunction, EMT, and Tissue Remodeling: A Possible Link between COPD and Lung Cancer. Biomed Res Int 2019;2019:2025636.
28. Barker TH, Dysart MM, Brown AC, et al. Synergistic effects of particulate matter and substrate stiffness on epithelial-to-mesenchymal transition. Res Rep Health Eff Inst 2014;(182):3-41.
29. Wang J, Huang J, Wang L, et al. Urban particulate matter triggers lung inflammation via the ROS-MAPK-NF-κB signaling pathway. J Thorac Dis 2017;9:4398-412.
30. Raju SM, Kumar AP, Yadav AN, et al. Haptoglobin improves acute phase response and endotoxin tolerance in response to bacterial LPS. Immunol Lett 2019;207:17-27.
31. Bullone M, de Lagarde M, Vargas A, et al. Serum Surfactant Protein D and Haptoglobin as Potential Biomarkers for Inflammatory Airway Disease in Horses. J Vet Intern Med 2015;29:1707-11.
32. Luo C, Li Y, Liang X, et al. Special electromagnetic field-treated water and far-infrared radiation alleviates lipopolysaccharide-induced acute respiratory distress syndrome in rats by regulating haptoglobin. Bioengineered 2021;12:6808-20.
33. Kerchberger VE, Bastarache JA, Shaver CM, et al. Haptoglobin-2 variant increases susceptibility to acute respiratory distress syndrome during sepsis. JCI Insight 2019;4:131206.
34. Wang Q, Shi Q, Liu L, et al. FGF10 mediates protective anti-oxidative effects in particulate matter-induced lung injury through Nrf2 and NF-κB signaling. Ann Transl Med 2022;10:1203.
35. Zhang G, Hou S, Li S, et al. Role of STAT3 in cancer cell epithelial-mesenchymal transition (Review). Int J Oncol 2024;64:48.
36. Liu H, Ren G, Wang T, et al. Aberrantly expressed Fra-1 by IL-6/STAT3 transactivation promotes colorectal cancer aggressiveness through epithelial-mesenchymal transition. Carcinogenesis 2015;36:459-68.
37. Lin CH, Wan C, Liu WS, et al. PM2.5 Induces Early Epithelial Mesenchymal Transition in Human Proximal Tubular Epithelial Cells through Activation of IL-6/STAT3 Pathway. Int J Mol Sci 2021;22:12734.
38. Cai S, Li N, Bai X, et al. ERK inactivation enhances stemness of NSCLC cells via promoting Slug-mediated epithelial-to-mesenchymal transition. Theranostics 2022;12:7051-66.
39. Guo H, Jian Z, Liu H, et al. TGF-β1-induced EMT activation via both Smad-dependent and MAPK signaling pathways in Cu-induced pulmonary fibrosis. Toxicol Appl Pharmacol 2021;418:115500.
40. Wang X, Aga EB, Tse WM, et al. Protective Effect of the Total Alkaloid Extract from Bulbus Fritillariae pallidiflorae in a Mouse Model of Cigarette Smoke-Induced Chronic Obstructive Pulmonary Disease. Int J Chron Obstruct Pulmon Dis 2024;19:1273-89.

(English Language Editor: J. Gray)

Cite this article as: Qian Y, Fang C, Wang B, Xu Z, Yu W, Gritsiuta AI, Chen C, Dong N, Chen J. Regulatory mechanisms of haptoglobin on particulate matter-induced epithelial-to-mesenchymal transition in bronchial epithelial cells. J Thorac Dis 2024;16(12):8724-8742. doi: 10.21037/jtd-2024-2013